Intermolecular Interactions at the Silica-Liquid Interface Modulate the Fermi Resonance Coupling in Surface Methanol

*Thomas T. Bui, Luis A. Colón, and Luis Velarde**

Department of Chemistry, University at Buffalo, State University of New York, Buffalo, NY 14260-3000

ABSTRACT.

The buried solid/liquid interface between hydrophilic fused silica and binary solvent mixtures of acetonitrile (MeCN) and methanol (MeOH) was studied with vibrational sum-frequency generation (vSFG) spectroscopy. Our data showed that at high relative concentrations of methanol, the Fermi resonance peak in the vSFG spectrum is greatly suppressed; progressively gaining intensity as methanol is diluted with perdeuterated acetonitrile. This phenomenon is quantified by the Fermi resonance coupling coefficient, *W*, extracted using a two-level model, as well as the experimental intensity ratio, R, of the methyl Fermi resonance band to that of the symmetric stretch. At a 1.0 MeOH mole fraction, *W* and R values were 10.3 ± 9.8 cm^{-1} and 0.01 ± 0.02, respectively, whereas at 0.1 mole fraction, *W* and R increased to 46.3 ± 3.6 cm^{-1} and 0.43 ± 0.16, respectively. This indicates that solvation with acetonitrile effectively tunes the Fermi coupling of methanol vibrations at the silica/liquid interface.

TOC GRAPHICS

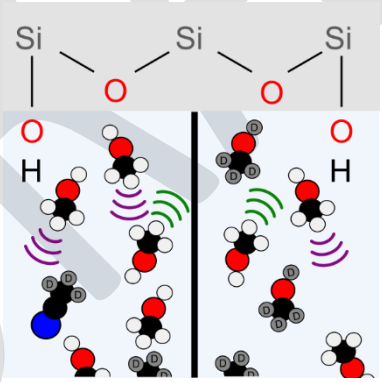

KEYWORDS Solid-liquid interfaces, silica surface, buried interfaces, binary mixtures, solvation, Fermi coupling.

The understanding of interfacial organization and intermolecular interactions in polar liquid binary mixtures, particularly acetonitrile and water, at hydrophilic silica surfaces has received renewed interest since hydrophilic interaction liquid chromatography (HILIC) came about as an alternative modality in high performance liquid chromatography (HPLC) for the chemical separation of polar analytes.[1-5] Analyte retention at the interface is attributed to a combination of partitioning of the analyte into a water-enriched surface layer due to favorable hydrogen bonding and electrostatic interactions. A complementary methodology is nonaqueous (NA)-HILIC, where alcohols, such as methanol, are used in place of water as the strong solvent (referring to its stronger attractive solvation forces with polar analytes) in mixtures with a weaker organic solvent, typically acetonitrile, as the mobile phase. Studies of analyte retention in NA-HILIC are sparse and, from a fundamental viewpoint, present a significant challenge considering that the *in-situ* characterization of the alcohol-rich stationary phase layer remains elusive. A lack of a molecular-level understanding regarding the contributing factors to the retention mechanism in various HILIC modalities has limited the advancement of this technique in liquid chromatography.[5] The structure of the ultrathin liquid interfacial layer over silica that acts as the stationary phase is dictated by a competing intermolecular interactions among solvent molecules and the silica surface functional groups. Such complexity at the solid/liquid surface has motivated experimental[6-9] and computational[10-15] studies to examine solvent partitioning and organization of binary solvent mixtures at the silica/liquid interface as model systems for HILIC.

Vibrational sum frequency generation (vSFG) spectroscopy is an optical second-order nonlinear spectroscopic technique that is effective in probing such buried interfaces without enduring largely interfering signals from the bulk.[16-19] Previous vSFG measurements of acetonitrile/water binary mixtures revealed that acetonitrile adsorbs at both hydrophilic and

hydrophobic quartz substrate.[6] The formation of a lipid-like antiparallel bilayer at the hydrophilic silica surface has been reported at concentrations as low as 10%,[7] with a clear pH dependence.[9]

Strong vSFG methanol bands appearing at ~2830, ~2920, and ~2945 cm^{-1} have been reported for the silica/vapor[8, 20] and liquid/vapor interfaces[21-29] and are attributed to the methyl symmetric stretching (r^+) and two Fermi resonance modes (r^+_{FR}), respectively. The peak assignment of the vSFG modes for methanol has been somewhat debated. Both the asymmetric stretching mode (r^-) and the r^+_{FR} mode have been assigned to the peak at ~2945 cm^{-1}.[30-31] However, polarization selection rules indicate that the r^+ and r^+_{FR} modes yield the greatest vSFG response in *ssp* polarization and the highest intensity for the r^- mode in *ppp* combination,[26] where *s* and *p* are representative of the light polarization for the SFG, visible, and infrared beams, respectively. Puzzlingly, the r^- mode, expected in the same energy region, has not been observed for any vSFG polarization combination for methanol at the silica/vapor interface[8, 20] nor liquid/vapor interface,[21-29] but has been detected on TiO_2 films.[32-36] However, according the bond additivity model,[37-38] the intensity of the r^- mode is expected to be significantly weaker than the r^+ mode in *ssp* polarization.[24]

In contrast, the vSFG signals of liquid methanol at the hydrophilic silica/liquid interface have remained elusive, with the reported signals showing no significant vibrational bands in the methyl stretching region (2800-3000 cm^{-1}).[6, 8, 14, 20, 39] This has been rationalized in terms of destructive interference effects from a well-ordered antiparallel double layer, where the hydroxyl group of methanol molecules directly at the interface and methanol molecules at a subsequent layer point in opposite directions leading to a net signal cancellation.[20] Later reports have attributed the lack of signal to dynamic effects and/or equal number of oppositely aligned interfacial methanol molecules.[8] The lack of signal response from methanol has hindered our understanding of the simplest alcohol at the silica/liquid interface, thus the interfacial interactions and dynamics of

methanol on the silica surface remain undetermined. Herein, we use nonlinear second-order vSFG spectroscopy to generate high signal-to-noise ratio spectra for the weak signals originating from the liquid/fused silica interface in order to elucidate relevant intermolecular interactions and partitioning for a series of binary MeOH/MeCN liquid mixtures at the fused silica surface.

Figure 1 reports the *ssp* vSFG spectrum of liquid MeOH at the fused silica interface. The figure shows a direct comparison of the interfacial C-H signal response from neat acetonitrile and neat methanol adsorbed onto an IR-grade fused silica substrate (Corning 7979 by Esco Optics, Inc.) obtained under the same experimental conditions. This result puts into perspective the drastic difference in the vSFG intensity between the two species, making it very understandable why previous attempts have reported a lack of vSFG signal from liquid methanol on silica. Methanol signals are nearly at the baseline level of the SiO_2/MeCN spectrum as shown in Figure 1a. The r^+ mode of MeCN appears at 2943.9 $\pm$ 0.2 cm^{-1}, in agreement with previous reports.[6-9] Shown in Figure 1b are the r^+ and two r^+_{FR} modes for MeOH detected at 2846.0 $\pm$ 0.3 cm^{-1}, 2910 $\pm$ 3.6 cm^{-1} and 2940.8 $\pm$ 5.2 cm^{-1}, respectively, and are in agreement with the well-known bands of methanol.[8, 21-23, 25, 27-29] The broad gradual rise in sum frequency signal at higher frequencies is attributed to O-H vibrations from the hydroxyl group of interfacial methanol as special care was taken to minimize the presence of water in the sample. For the remainder of this letter, we focus our discussion in the C-H vibrational region. It is important that to obtain the best alignment at the solid/liquid interface, a spot of gold (sufficiently far away from the sampling region) was added to the fused silica substrates (on the side facing the liquid) to serve as a reference for SFG optimization as it generates a large non-resonant signal as described by Barret and Petersen.[40]

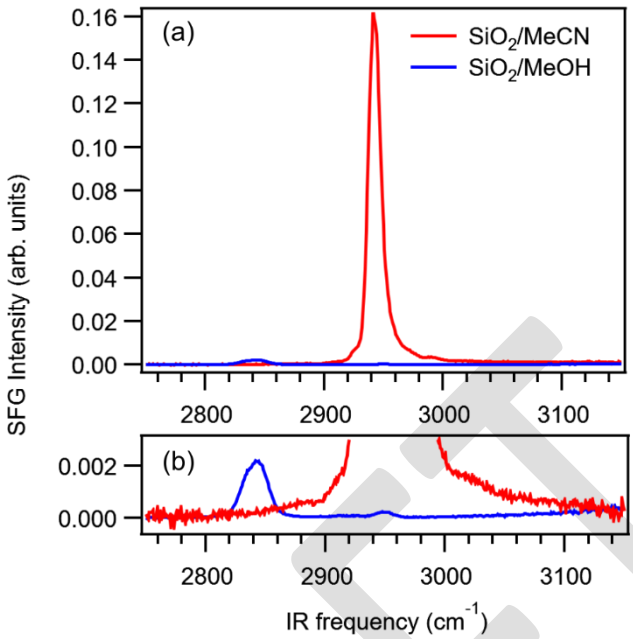

Figure 1. vSFG signal response of acetonitrile (red) and methanol (blue) acquired in *ssp* polarization at the silica/liquid interface obtain under the same experimental conditions. (a) Direct comparison of the normalized intensities obtained for the neat MeCN and neat MeOH solid/liquid vSFG spectra. (b) Magnified plot from the data in Figure 1a showing the MeOH spectral details.

Although the peak positions agree with previous reports of interfacial MeOH, the intensity of the Fermi resonance peaks appear to be vastly weaker than what has been reported for other interfaces, such as the silica/vapor. However, it is important to note that our measurements showed a strong dependence of the Fermi resonance intensity with the type of SiO_2 substrate and pretreatment procedure. For instance, neat methanol showed a clear difference in intensity for the r^{+}_{FR} mode at 2940.8 $\pm$ 5.2 cm^{-1} on IR fused silica (Corning 7979) used in this study compared to our results on fused quartz (GE 124) shown in Figure S2. The OH content is known to be less for fused quartz compared to fused silica, and we tentatively attribute the distinct Fermi resonance intensities to different silanol population and crystallinity between the two substrates. Differences in silica pretreatment[41] , as well as the type of substrate for the TiO_2 case,[42] have shown to affect spectral bands of neat water and vapor methanol, respectively. Density profiles of water on quartz

compared to on fused silica surfaces have shown to differ in its structural layers as well.[43] It is also important to note that prior to our experiments (see Supporting Information for details of sample preparation), fused silica windows were UV-ozone treated for the removal of any organic contaminants, which is known to increase the number of free silanol and siloxane surface groups.[44] Here, we discuss only the results using fused silica substrates as fused silica is more commonly used in chromatography applications. The results and differences regarding fused quartz will be addressed in a later study.

One of the advantages of being able to detect methanol at the solid/liquid interface is that a series of binary solvent mixtures of MeOH with perdeuterated MeOH-d4 or MeCN-d3, could be systematically studied in order to gain fundamental insights into the interfacial solvation effects on the molecular organization and competing interactions of methanol at the silica surface. We also prepared MeCN mixtures with MeOH-d4 at varying mole fractions. While some exchange of hydrogen and deuterium (H/D exchange) in the alkyl groups might be considered, the alkyl C–H bonds are relatively inert towards H/D exchange without a catalyst to activate these bonds, allowing us to draw conclusions in terms of solvation.

Figures 2a.1 and 2b.1 are the vSFG experimental spectra of MeCN/MeOH-d4 and MeOH/MeOH-d4 probed at varying mole fractions, respectively. Our measurements for MeCN/MeOH-d4 in Figure 2a.1 are in agreement with previous experimental reports, where the maximum intensity observed for the r^+ mode is not observed at 100% but rather at ~90% (Figure 2a.4 and 2a.5), and a decrease for mole percentages smaller than ~90%.[8] The decrease in intensity at lower mole fractions is attributed to a decrease in number density of molecules at the interface, whereas the decrease beyond ~90% has been attributed to signal cancelation due to antiparallel bilayer ordering of acetonitrile molecules in the interfacial region. Although it is expected that the

coherent sum frequency responses of opposite phase cancel out for transition dipoles of the same vibrational mode pointing in opposite direction,[45] the cancelation here is not perfect as the signal persists at the highest and lowest concentrations of MeCN due to a frequency shift between the molecules pointing towards the liquid (peak 1 in Figure 2a.2) and the leaflet interacting with the silica (peak 2 in Figure 2a.2),[10] creating therefore an asymmetric solvation environment at the interface.

Interestingly, a similar Mountain plot[11] trend is observed for MeOH, where the maximum signal appears at ~80% and then decreases at higher concentrations as shown in Figures 2b.1, 2b.4, and 2b.5. The signals from methanol are significantly weaker compared to acetonitrile with lower signal to noise ratios. The r^+ mode and r^+_{FR} modes for hydrogenated MeOH are not observable until approximately ~20% and ~60%, respectively. MeOH samples below 20% are unfortunately below our limits of detection, most likely due to a combination of the methanol weak SFG response and lower surface coverage as hydrogenated methanol and its deuterated form should have no preference, relative to each other, for the silica surface (analogous surface affinity). Similar to the acetonitrile case, we attribute the rise in intensity between 20-80% to the increase in number density of methanol molecules at the surface. The decrease in intensity at higher mole percent (> 80%) agrees with previous reports at the liquid/vapor interface.[22-23, 27-29] It remains a mystery why the vSFG signals of interfacial liquid MeOH are so much weaker than those of liquid MeCN. Li et al., has proposed that the decrease in intensity at higher concentrations are due to the decrease in the Raman polarizability and IR transition dipole component to the microscopic hyperpolarizability tensor.[27] Molecular dynamics (MD) calculations have shown that surface defects can increase the population of methanol in the second sublayer with opposing orientations to methanol at the surface, resulting in a decrease of the r^+ mode vSFG signal.[14] Interestingly, the

weaker r^{+}_{FR} mode is almost undetectable until ~60% MeOH/MeOH-d4 increasing modestly with increasing mole fractions or methanol molecules at the interface.

Experimental evidence for a double layer of acetonitrile in water mixtures has been supported, in part, by using two opposite phase Lorentzian functions spaced by ~11 cm^{-1} to fit the r^{+} mode.[7] Here, we report our fittings with one and two Lorentzian function(s) as demonstrated in Figures 2a.2 and 2b.2 for 80% dilutions of both MeCN and MeOH, respectively, with MeOH-d4. For both MeCN and MeOH cases, peak 1 (lower-frequency) is attributed to the r^{+} mode in the second sublayer, and peak 2 (higher-frequency) corresponds to the r^{+} mode of solvents closest to the silica surface. The fits with two peaks show consistently a better agreement indicated by the residual. The higher-frequency resonance for the first sublayer reveals a blue-shift induced by hydrogen bonding to the substrate. The frequency separation of the two Lorentzian functions for the r^{+} mode, obtained in our fits, averaged to be 12 cm^{-1}, well in agreement with what has been reported for acetonitrile at the silica/liquid interface.[7]

The formation of an antiparallel double layer for liquid methanol is currently debated and computational studies suggest an absence of a typical double layer formation for methanol at the silica/liquid interface.[12-14] Our Lorentzian fits indicate that oppositely phased methanol contributions do a better job representing the data as supported by the residual plots in Figure 2b.3 for MeOH/MeOH-d4. A rare case when the hydrophobic tail of methanol points towards silica at the surface may also be possible as hydrophobic patches are known to exist at the surface of hydrophilic silica surfaces.[46-49] Depending on the pretreatment of silica substrates, silanol may dehydroxylate to partly hydrophobic siloxane groups.[41, 44] Another scenario for the non-single Lorentzian lineshape may arise from inhomogeneous broadening contributions and this needs to be further explored with high resolution lineshape sensitive methods.[50] While fitting with a Voigt

function that accounts for the instrument response was superior than the one Lorentzian fit, the two peak model was somewhat better reproducing our spectral lineshape satisfactorily. This question is worth revisiting with higher spectral resolution and improved signal-to-noise ratios (section 2 of the SI).

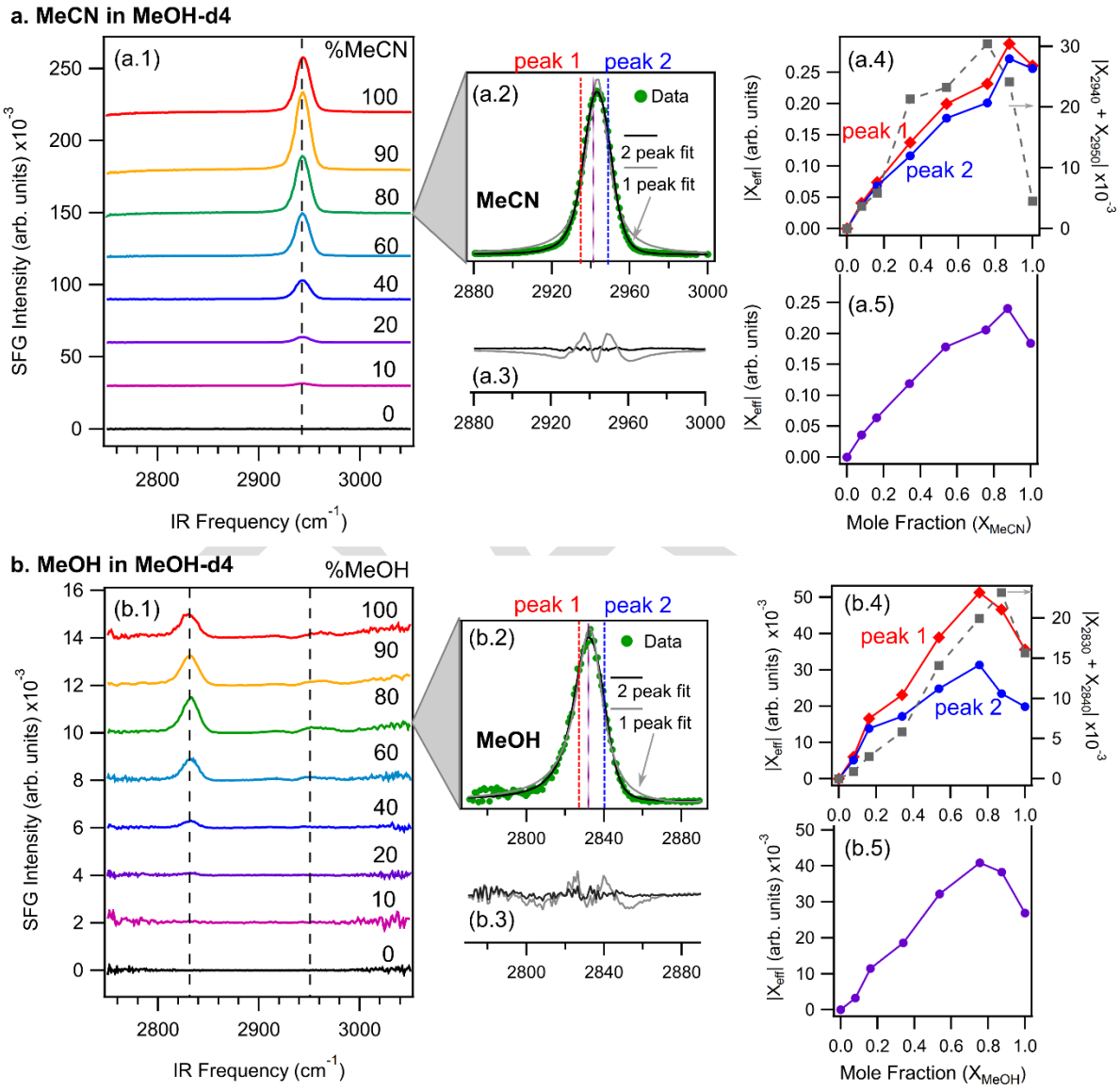

Figure 2. vSFG spectra of binary solvent mixtures of MeCN and MeOH with deuterated methanol at varying mole percent (a.1 and b.1, respectively). The spectra are offset for clarity. The methyl symmetric stretching mode for both MeCN and MeOH fit to one (grey) and two (black) Lorentzian function(s) (a.2 and b.2, respectively), along with fitting residuals (a.3 and b.3, respectively). The amplitudes (left axis) of the Lorentzian functions for two peaks (red diamonds and blue circles) are plotted as a function of increasing mole fraction for MeCN and MeOH (a.4 and b.4, respectively) as well as the sum of the two

oppositely phased methyl peak amplitude (grey squares, right axis). The intensities of MeCN and MeOH arising from $|\chi_{eff}|$ for a one peak Lorentzian function (purple) are plotted against the mole fraction (a.5 and b.5, respectively). The lines for peak 1, 2, and sum amplitudes and intensities from $|\chi_{eff}|$ are a guide for the eye.

Figures 2a.4 and 2b.4 display the respective fitted amplitudes for the two Lorentzians, as well as the absolute square of the sum of the oppositely phased complex Lorentzians. Although it is clear that two Lorentzian functions produce more accurate fits (for both MeCN/MeOH-d4 and MeOH/MeOH-d4), the fit results with a single Lorentzian provide similar overall trends as shown in Figures 2 a.4-a.5 and b.4-b.5. Figure 2a.5 is greatly in agreement with what has been reported previously,[8] as well as with the calculations by Mountain.[11] This rules out potential overfitting as the source of this phenomena.

To gain further insight into the effects of local intermolecular interactions on the unusual Fermi resonance coupling strength observed for the methyl group in liquid methanol at the silica surface, samples of hydrogenated methanol in per-deuterated acetonitrile (MeCN-d3) were prepared at varying mole fractions. From Figure 3a, it is evident that there are significant differences in the SFG spectral lineshapes between the MeOH/MeCN-d3 results and the MeOH/MeOH-d4 measurements in Figure 2b.1. The r^{+}_{FR} band for the MeOH/MeCN-d3 dilutions gradually increases (relatively to the r^{+} peak) as the bulk methanol concentration is lowered. In sharp contrast with the MeOH/MeOH-d4 mixtures where the r^{+}_{FR} mode is significantly suppressed at all concentrations (Figure 2b.1). Such different r^{+}_{FR} intensity dependence between the two cases suggests a direct link between this band and neighboring intermolecular interactions at the interface.[51] The silica surface has no preference for either hydrogenated or deuterated methanol molecules, therefore both isotopologues will compete for available surface adsorption sites. However, methanol is known to preferentially adsorb to the silica surface over acetonitrile through favorable hydrogen bonding with the silica surface groups. Methanol in closest proximity to the

silica surface forms a hydrophobic layer with terminal methyl groups pointing towards the liquid phase.[15] Through van der Waals forces, the methyl groups of this first layer will affect the orientation of subsequent layers. MD studies show that this hydrophobic layer does not discriminate between methanol and acetonitrile in the subsequent layer, as this is dictated by comparable methyl-methyl interactions.[12]

It is known that oppositely phased methanol in a second layer can decrease the observed r^+ mode SFG signal for higher MeOH concentrations, however, the r^+_{FR} band of interfacial methanol may also be suppressed from the destructive interference resulting from an the antiparallel configuration. Due to such coherent signal cancellation from oppositely phased methanol molecules, two Lorentzian functions for both oppositely phased r^+ and corresponding r^+_{FR} bands works best to accommodate a model for both methanol closest to the silica surface and methanol in the subsequent layer. Here, we refer to the higher-frequency r^+ and r^+_{FR} pairs from our two oppositely phased Lorentzian fitting as methanol closest to the silica surface, and the lower-frequency r^+ and r^+_{FR} pair as methanol in the second sublayer. For the r^+ band, these are shown as peak 2 and peak 1 in Figure 2, respectively. The comparison of r^+ amplitudes fitted to one methyl and two Lorentzian functions for the MeOH/MeCN-d3 dilutions are shown in Figure S3 as a reference.

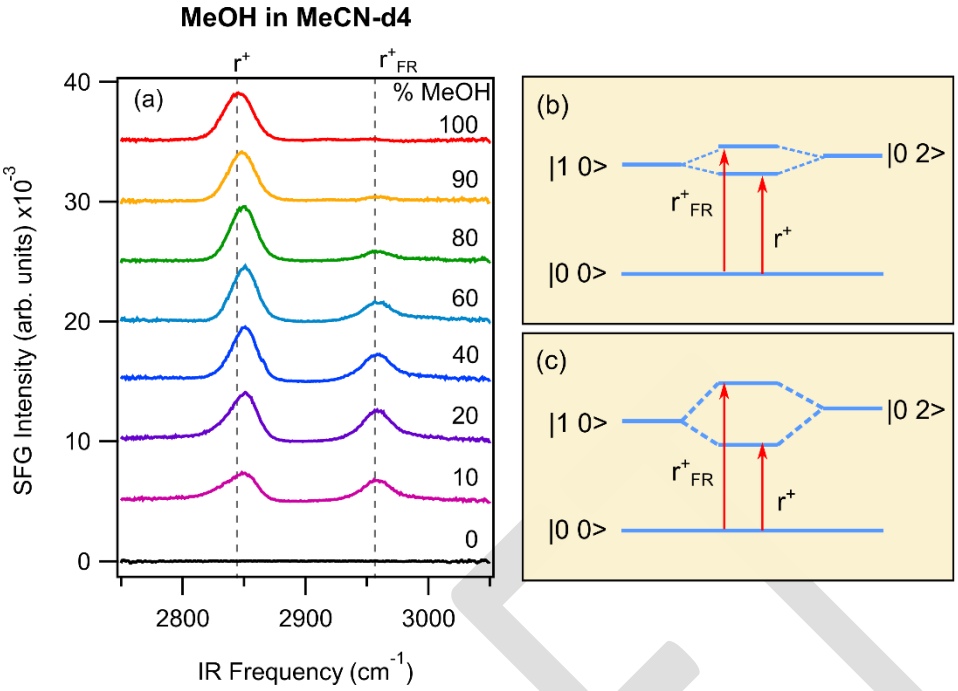

Figure 3. vSFG spectra of methanol with deuterated acetonitrile at varying mole percent (a). Spectra are offset for clarity. Energy diagrams depicting the molecular coupling/de-coupling between the r^+ and r^+_{FR} modes at high (b) and low (c) concentrations of MeOH.

It is evident that with decreasing MeOH concentrations, both dominant modes appear to blue shift in what looks like a solvatochromic effect induced by more MeCN molecules in the solvation shell (see Figure 3). For example, for bulk binary mixtures of carbon disulfide in benzene, a blue-shift is observed for the fundamental mode (ν_1) and Fermi resonance mode ($2\nu_2$) of carbon disulfide with decreasing concentrations.[52-54] For liquid methanol at the silica interface, we observed a blue-shift with decreasing MeOH concentration for the r^+_{FR} band at 2945 cm^{-1} as well as in our Raman measurements of MeOH/MeCN-d3 as shown in Figure S4. However, the Raman intensity of the r^+_{FR} mode decreases proportionally with decreasing MeOH concentration in the bulk measurements, whereas at the interface the vSFG intensity clearly increases as shown in Figure 3a. This suggests that the *Fermi resonance coupling strength is not only affected by bulk*

solvation but it is uniquely sensitive to the nearby surface chemical composition as well as interfacial organization and local solvation environment. Figures 3b and 3c display schematic energy-level diagrams to visualize the changes in Fermi resonance coupling strength at high and low MeOH concentrations, respectively. At high MeOH concentrations, Fermi coupling in interfacial molecules appears to be weaker, with the r^{+}_{FR} mode borrowing less intensity from the fundamental mode as indicated by the low Fermi signal for a MeOH/MeCN-d3 mole fraction of 1.0. This stronger coupling is also supported by an increased frequency difference between the r^{+} and r^{+}_{FR} bands from pure MeOH to the MeOH/MeCN-d3 dilutions as shown in tables S3 and S4. However, the splitting due to Fermi coupling is also convoluted with solvatochromic shifts in our study and below we describe better metrics to quantify this phenomenon.

Recent reports have shown that the intermolecular interactions of neighboring molecules at the interface may be quantified by the SFG intensity ratio of the Fermi resonance and the methyl symmetric stretch.[55-58] For instance, Tian et al., have established a method to deduce the total intermolecular interactions of phospholipids in a monolayer by relating it to the second-order Fermi resonant signal.[57] A relationship between the intensity ratio, R, of the Fermi resonant mode and methyl stretching mode, established an effective method to relate increasing neighboring phospholipids interactions to the Fermi coupling strength with increasing surface pressure. Figure 4a displays R values for MeOH/MeCN-d3 mixtures from the higher-frequency r^{+} and r^{+}_{FR} peak fits using two Lorentzian functions using the calculated R values according to Eq. S2 and listed in Table S1. As the concentration of MeOH increases, the R value monotonically declines. This suggests that the intensity of the r^{+}_{FR} mode of MeOH is coupled to the interactions with neighboring molecules at the silica surface. At the solid/liquid interface this correlation may be more intricate than simply a relative bulk concentration dependance for binary mixtures, as

methanol will preferentially adsorb to the silica surface over acetonitrile, covering the surface even at low mole fractions.[13]

Figure 4b shows the R values plotted with the mole fractions for MeOH/MeOH-d4 mixtures using the higher-frequency r^+ and r^+_{FR} peak fits from two Lorentzian functions. No clear relationship between the calculated R ratio values and relative MeOH concentration is observed. This strongly advocates for the distinctive intermolecular interactions with the MeCN-d3 molecules at the interface as the cause of the R value dependence in Figure 4a. The difference between the contrasting responses for MeOH/MeOH-d4 and MeOH/MeCN-d3 mixtures are likely to arise due to the unique energetic shiftings due to solvation effects at the silica interface and not merely a concentration effect. Interestingly, while the one peak fit results behave similarly to the higher-frequency trends reported in Figure 4, we determined that the R values obtained for methanol in the second layer (lower-frequency band in the two peak fit) do not show an evident relationship to the Fermi resonance coupling with respect to dilutions in either case. This indicating that the second methanol layer occurs mostly in MeOH patches where local intermolecular interactions remain distinct from regions in the second sublayer displaced by MeCN. Figures S5a and S5b show the calculated R values for MeOH/MeCN-d3 and MeOH/MeOH-d4 mixtures obtained from the lower-frequency r^+ and r^+_{FR} peak fits using two Lorentzian functions, respectively and the calculated R values can be found in Table S2.

To further deduce the Fermi resonance coupling effect observed at an interface for MeOH/MeCN-d3, we use the well-established two-level model in order to help quantify the effects of varying the methanol concentration on Fermi resonance coupling coefficient, W.[42, 58-60] The theory for the model has been described in previous reports for liquid methanol,[42, 59-60] and it is summarized in the supporting information along with the calculated W for various mole fractions

using the higher-frequency (first sublayer), r^+ and r^+_{FR} values from two Lorentzian functions listed in Table S1. The Fermi resonance coupling coefficient quantifies the coupling strength of two nearly degenerate states. Hou et al., have applied this model in order to support their results that the Fermi resonance mode is more suppressed at the SiO_2/CH_3CD_2OH ($W = 25 \pm 2$ cm^{-1}) interface than for CaF_2/CH_3CD_2OH ($W = 30 \pm 1$ cm^{-1}).[58] Figure 4c displays our calculated Fermi resonance coupling coefficients plotted as a function of increasing MeOH mole fraction for MeOH/MeCN-d3 mixtures. It can be seen that as the relative MeOH concentration rises, *W* decreases, supporting the case for the r^+_{FR} mode being suppressed at higher MeOH concentrations. At 0.1 MeOH/MeCN-d3 mole fraction the Fermi coupling strength is $W = 46.3 \pm 3.6$ cm^{-1}, whereas the Fermi coupling coefficient for the 1.0 MeOH mole fraction was calculated to be only 10.3 ± 9.8 cm^{-1}. Calculated R and *W* values using one and two r^+ with a single r^+_{FR} Lorentzian function revealed comparable trends as shown in Figures S6 and S7, respectively, showing that these trends are not a result of possible overfitting. The only difference being the lower-frequency bands in the two peak model as discussed above.

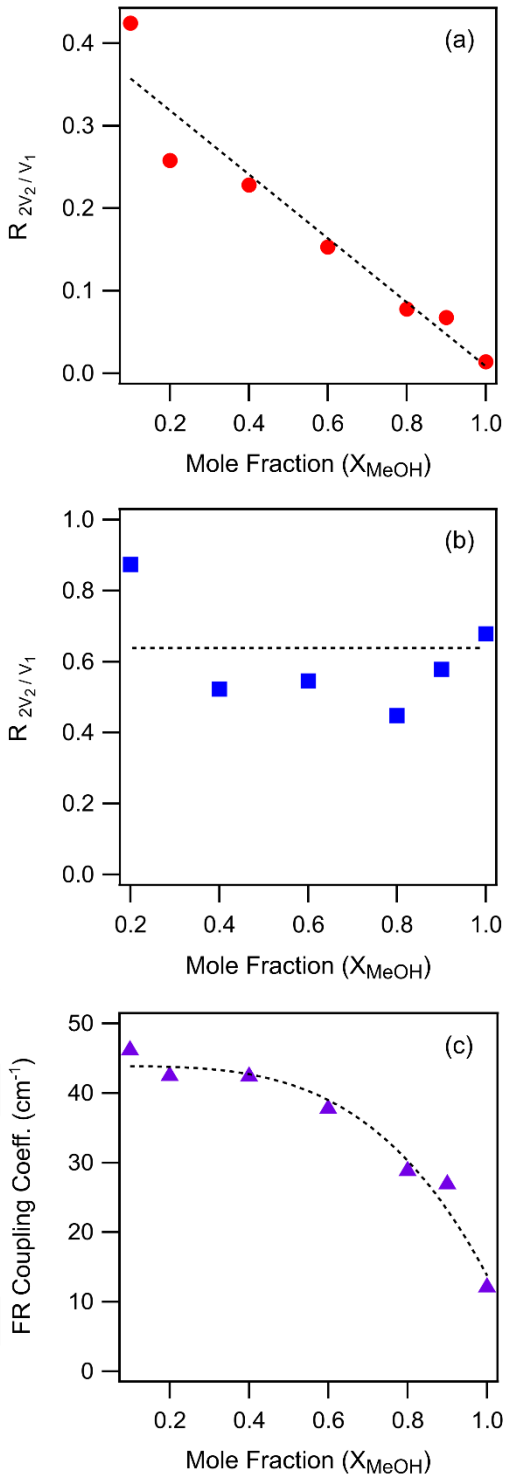

Figure 4. Intensity ratios (R_{2V_2/V_1}) of methanol at the silica/liquid interface plotted as a function of increasing MeOH concentrations for binary mixtures of MeOH in MeCN-d3 (a) and MeOH in MeOH-d4 (b). Fermi resonance coupling coefficients (*W*) are plotted vs. increasing methanol mole fractions for MeOH/MeCN-d3 on hydrophilic fused silica (c). Dashed lines are a guide for the eye.

It is important to note that initially, we carried out both MeOH/MeOH-d4 and MeOH/MeCN-d3 experiments starting with 1.0 MeOH mole fraction and observed that methanol strongly "sticks" to the silica surface and the methyl CH stretching bands of methanol appeared for the last 0.0 MeOH mole fraction sample after flushing the cell several times with the 0.0 MeOH solution. Details of the experimental sample preparation can be found in the supporting information. These results are somewhat analogous to what was observed for α-pinene adsorbed to fused silica, where SFG signals of α-pinene vapor/He flow remained after alternating to pure He flow.[61] Despite these surprising results from our initial trial starting with 1.0 and ending with 0.0 MeOH mole fraction, we obtained similar trends for the r^{+}_{FR} mode intensity trends, namely being suppressed at high MeOH concentrations and increased at lower MeOH concentrations. Therefore, experimental sampling order did not affect the results and conclusions presented here. Importantly, MeOH/D_2O mixtures on hydrophilic fused silica were measured to study the effects of silica surface hydration on the Fermi coupling strength. Further investigation is ongoing but preliminary results indicate that hydration has an effect on the Fermi peak as well (Figure S8).

In summary, we showed that the elusive vSFG signals from methanol at the silica/liquid interface are exceedingly weaker than acetonitrile but are detectable with sufficient sensitivity. The symmetric stretch intensity trends of both MeCN/MeOH-d4 and MeOH/MeOH-d4 mixtures follows the trend previously reported for MeCN/H_2O with increasing MeCN and MeOH concentrations, respectively. However, MeOH/MeCN-d3 mixtures reveal distinctive spectral trends, especially regarding the Fermi coupling strength of the methyl group. We conclude that the Fermi coupling strength is highly sensitive to the SiO_2 surface composition along with local solvation effects which will be elaborated in a future work. The weak intensity of the r^{+}_{FR} mode observed at higher methanol concentrations on fused silica suggests that neighboring methanol

molecules at the interface suppress the Fermi coupling. This is supported by calculated R and *W* parameters as a function of mole fraction. The work here demonstrates the unique capabilities of vibrational sum frequency lineshapes to obtain insights on interfacial behavior even for extremely weak signals and shed light on unique phenomena at solid/liquid interfaces.

SUPPORTING INFORMATION

Detailed experimental methods, curve fittings and analysis, fused quartz substrate results, Raman spectra, effects of D_2O exposure.

ACKNOWLEDGMENTS

This work was supported by the National Science Foundation under award no. CHE-1753207.

AUTHOR INFORMATION

Corresponding Author: *lvelarde@buffalo.edu

REFERENCES

1. Alpert, A. J. Hydrophilic-interaction chromatography for the separation of peptides, nucleic acids and other polar compounds. *J. Chromatogr. A* **1990,** *499*, 177-196.
2. Hemström, P.; Irgum, K. Hydrophilic interaction chromatography. *J. Sep. Sci.* **2006,** *29*, 1784-1821.
3. Boersema, P. J.; Mohammed, S.; Heck, A. J. R. Hydrophilic interaction liquid chromatography (HILIC) in proteomics. *Anal. Bioanal. Chem.* **2008,** *391*, 151-159.

4. Gong, L.; McCullagh, J. S. O. Analysis of oligonucleotides by hydrophilic interaction liquid chromatography coupled to negative ion electrospray ionization mass spectrometry. *J. Chromatogr. A* **2011,** *1218*, 5480-5486.
5. Buszewski, B.; Noga, S. Hydrophilic interaction liquid chromatography (HILIC)—a powerful separation technique. *Anal. Bioanal. Chem.* **2012,** *402*, 231-247.
6. Henry, M. C.; Piagessi, E. A.; Zesotarski, J. C.; Messmer, M. C. Sum-Frequency Observation of Solvent Structure at Model Chromatographic Interfaces: Acetonitrile−Water and Methanol−Water Systems. *Langmuir* **2005,** *21*, 6521-6526.
7. Rivera, C. A.; Bender, J. S.; Manfred, K.; Fourkas, J. T. Persistence of Acetonitrile Bilayers at the Interface of Acetonitrile/Water Mixtures with Silica. *J. Phys. Chem. A* **2013,** *117*, 12060-12066.
8. Gobrogge, E. A.; Walker, R. A. Binary Solvent Organization at Silica/Liquid Interfaces: Preferential Ordering in Acetonitrile–Methanol Mixtures. *J. Phys. Chem. Lett.* **2014,** *5*, 2688-2693.
9. Rehl, B.; Li, Z.; Gibbs, J. M. Influence of High pH on the Organization of Acetonitrile at the Silica/Water Interface Studied by Sum Frequency Generation Spectroscopy. *Langmuir* **2018,** *34*, 4445-4454.
10. Ding, F.; Hu, Z.; Zhong, Q.; Manfred, K.; Gattass, R. R.; Brindza, M. R.; Fourkas, J. T.; Walker, R. A.; Weeks, J. D. Interfacial Organization of Acetonitrile: Simulation and Experiment. *J. Phys. Chem. C* **2010,** *114*, 17651-17659.
11. Mountain, R. D. Molecular Dynamics Simulation of Water–Acetonitrile Mixtures in a Silica Slit. *J. Phys. Chem. C* **2013,** *117*, 3923-3929.
12. Melnikov, S. M.; Höltzel, A.; Seidel-Morgenstern, A.; Tallarek, U. Evaluation of Aqueous and Nonaqueous Binary Solvent Mixtures as Mobile Phase Alternatives to Water–Acetonitrile Mixtures for Hydrophilic Interaction Liquid Chromatography by Molecular Dynamics Simulations. *J. Phys. Chem. C* **2015,** *119*, 512-523.
13. Karnes, J. J.; Benjamin, I. Mechanism and Dynamics of Molecular Exchange at the Silica/Binary Solvent Mixtures Interface. *J. Phys. Chem. A* **2015,** *119*, 12073-12081.
14. Karnes, J. J.; Gobrogge, E. A.; Walker, R. A.; Benjamin, I. Unusual Structure and Dynamics at Silica/Methanol and Silica/Ethanol Interfaces—A Molecular Dynamics and Nonlinear Optical Study. *J. Phys. Chem. B* **2016,** *120*, 1569-1578.
15. Roy, D.; Liu, S.; Woods, B. L.; Siler, A. R.; Fourkas, J. T.; Weeks, J. D.; Walker, R. A. Nonpolar Adsorption at the Silica/Methanol Interface: Surface Mediated Polarity and Solvent Density across a Strongly Associating Solid/Liquid Boundary. *J. Phys. Chem. C* **2013,** *117*, 27052-27061.
16. Eisenthal, K. B. Liquid Interfaces Probed by Second-Harmonic and Sum-Frequency Spectroscopy. *Chem. Rev.* **1996,** *96*, 1343-1360.
17. Wei, X.; Hong, S.-C.; Zhuang, X.; Goto, T.; Shen, Y. R. Nonlinear optical studies of liquid crystal alignment on a rubbed polyvinyl alcohol surface. *Phys. Rev. E* **2000,** *62*, 5160-5172.
18. Shen, Y. R.; Ostroverkhov, V. Sum-Frequency Vibrational Spectroscopy on Water Interfaces: Polar Orientation of Water Molecules at Interfaces. *Chem. Rev.* **2006,** *106*, 1140-1154.
19. Wang, H.-F.; Velarde, L.; Gan, W.; Fu, L. Quantitative Sum-Frequency Generation Vibrational Spectroscopy of Molecular Surfaces and Interfaces: Lineshape, Polarization, and Orientation. *Annu. Rev. Phys. Chem.* **2015,** *66*, 189-216.
20. Liu, W.; Zhang, L.; Shen, Y. R. Interfacial layer structure at alcohol/silica interfaces probed by sum-frequency vibrational spectroscopy. *Chem. Phys. Lett.* **2005,** *412*, 206-209.

21. Superfine, R.; Huang, J. Y.; Shen, Y. R. Nonlinear optical studies of the pure liquid/vapor interface: Vibrational spectra and polar ordering. *Phys. Rev. Lett.* **1991,** *66*, 1066-1069.
22. Ma, G.; Allen, H. C. Surface Studies of Aqueous Methanol Solutions by Vibrational Broad Bandwidth Sum Frequency Generation Spectroscopy. *J. Phys. Chem. B* **2003,** *107*, 6343-6349.
23. Chen, H.; Gan, W.; Lu, R.; Guo, Y.; Wang, H.-f. Determination of Structure and Energetics for Gibbs Surface Adsorption Layers of Binary Liquid Mixture 2. Methanol + Water. *J. Phys. Chem. B* **2005,** *109*, 8064-8075.
24. Wu, H.; Zhang, W.-k.; Gan, W.; Cui, Z.-f.; Wang, H.-f. An empirical approach to the bond additivity model in quantitative interpretation of sum frequency generation vibrational spectra. *J. Chem. Phys.* **2006,** *125*, 133203.
25. Gan, W.; Wu, B.-h.; Zhang, Z.; Guo, Y.; Wang, H.-f. Vibrational Spectra and Molecular Orientation with Experimental Configuration Analysis in Surface Sum Frequency Generation (SFG). *J. Phys. Chem. C* **2007,** *111*, 8716-8725.
26. Lu, R.; Gan, W.; Wu, B.-h.; Zhang, Z.; Guo, Y.; Wang, H.-f. C−H Stretching Vibrations of Methyl, Methylene and Methine Groups at the Vapor/Alcohol (n = 1−8) Interfaces. *J. Phys. Chem. B* **2005,** *109*, 14118-14129.
27. Li, X.; Liu, J.; Lin, K.; Zhang, Y.; Zhang, Y.; Zheng, R.; Shi, Q.; Guo, Y.; Lu, Z. Toward Unraveling the Puzzle of Sum Frequency Generation Spectra at Interface of Aqueous Methanol Solution: Effects of Concentration-Dependent Hyperpolarizability. *J. Phys. Chem. C* **2019,** *123*, 12975-12983.
28. Wolfrum, K.; Graener, H.; Laubereau, A. Sum-frequency vibrational spectroscopy at the liquid—air interface of methanol. Water solutions. *Chem. Phys. Lett.* **1993,** *213*, 41-46.
29. Sung, J.; Park, K.; Kim, D. Surfaces of Alcohol−Water Mixtures Studied by Sum-Frequency Generation Vibrational Spectroscopy. *J. Phys. Chem. B* **2005,** *109*, 18507-18514.
30. Iwaki, L. K.; Dlott, D. D. Ultrafast vibrational energy redistribution within C–H and O–H stretching modes of liquid methanol. *Chem. Phys. Lett.* **2000,** *321*, 419-425.
31. Dlott, D. D. Vibrational energy redistribution in polyatomic liquids: 3D infrared–Raman spectroscopy. *Chem. Phys.* **2001,** *266*, 149-166.
32. Wang, C.-y.; Groenzin, H.; Shultz, M. J. Surface Characterization of Nanoscale TiO2 Film by Sum Frequency Generation Using Methanol as a Molecular Probe. *J. Phys. Chem. B* **2004,** *108*, 265-272.
33. Wang, C.-y.; Groenzin, H.; Shultz, M. J. Comparative Study of Acetic Acid, Methanol, and Water Adsorbed on Anatase TiO_2 Probed by Sum Frequency Generation Spectroscopy. *J. Am. Chem. Soc.* **2005,** *127*, 9736-9744.
34. Liu, A.-a.; Liu, S.; Zhang, R.; Ren, Z. Spectral Identification of Methanol on TiO_2(110) Surfaces with Sum Frequency Generation in the C–H Stretching Region. *J. Phys. Chem. C* **2015,** *119*, 23486-23494.
35. Peng, X.; Zhang, R.; Feng, R.-r.; Liu, A.-a.; Zhou, C.; Guo, Q.; Yang, X.; Jiang, Y.; Ren, Z. Active Species in Photocatalytic Reactions of Methanol on TiO_2(110) Identified by Surface Sum Frequency Generation Vibrational Spectroscopy. *J. Phys. Chem. C* **2019,** *123*, 13789-13794.
36. Zhang, R.; Wang, H.; Peng, X.; Feng, R.-r.; Liu, A.-a.; Guo, Q.; Zhou, C.; Ma, Z.; Yang, X.; Jiang, Y.; Ren, Z. In Situ Studies on Temperature-Dependent Photocatalytic Reactions of Methanol on TiO_2(110). *J. Phys. Chem. C* **2019,** *123*, 9993-9999.
37. Hirose, C.; Akamatsu, N.; Domen, K. Formulas for the analysis of surface sum-frequency generation spectrum by CH stretching modes of methyl and methylene groups. *J. Chem. Phys.* **1992,** *96*, 997-1004.

38. Hirose, C.; Yamamoto, H.; Akamatsu, N.; Domen, K. Orientation analysis by simulation of vibrational sum frequency generation spectrum: CH stretching bands of the methyl group. *J. Phys. Chem.* **1993,** *97*, 10064-10069.
39. Zhang, L.; Liu, W.; Shen, Y. R.; Cahill, D. G. Competitive Molecular Adsorption at Liquid/Solid Interfaces: A Study by Sum-Frequency Vibrational Spectroscopy. *J. Phys. Chem. C* **2007,** *111*, 2069-2076.
40. Barrett, A.; Petersen, P. B. Order of dry and wet mixed-length self-assembled monolayers. *J. Phys. Chem. C* **2015,** *119*, 23943-23950.
41. Dalstein, L.; Potapova, E.; Tyrode, E. The elusive silica/water interface: isolated silanols under water as revealed by vibrational sum frequency spectroscopy. *Phys. Chem. Chem. Phys.* **2017,** *19*, 10343-10349.
42. Yang, D.; Li, Y.; Liu, X.; Cao, Y.; Gao, Y.; Shen, Y. R.; Liu, W.-T. Facet-specific interaction between methanol and TiO₂ probed by sum-frequency vibrational spectroscopy. *Proc. Natl. Acad. Sci. U.S.A.* **2018,** *115*, E3888.
43. Pezzotti, S.; Galimberti, D. R.; Gaigeot, M.-P. Deconvolution of BIL-SFG and DL-SFG spectroscopic signals reveals order/disorder of water at the elusive aqueous silica interface. *Phys. Chem. Chem. Phys.* **2019,** *21*, 22188-22202.
44. Clark, T.; Ruiz, J. D.; Fan, H.; Brinker, C. J.; Swanson, B. I.; Parikh, A. N. A New Application of UV−Ozone Treatment in the Preparation of Substrate-Supported, Mesoporous Thin Films. *Chem. Mater.* **2000,** *12*, 3879-3884.
45. Algoul, S. T.; Sengupta, S.; Bui, T. T.; Velarde, L. Tuning the Surface Ordering of Self-Assembled Ionic Surfactants on Semiconducting Single-Walled Carbon Nanotubes: Concentration, Tube Diameter, and Counterions. *Langmuir* **2018,** *34*, 9279-9288.
46. Cyran, J. D.; Donovan, M. A.; Vollmer, D.; Siro Brigiano, F.; Pezzotti, S.; Galimberti, D. R.; Gaigeot, M.-P.; Bonn, M.; Backus, E. H. G. Molecular hydrophobicity at a macroscopically hydrophilic surface. *Proc. Natl. Acad. Sci. U.S.A.* **2019,** *116*, 1520.
47. Isaienko, O.; Borguet, E. Hydrophobicity of Hydroxylated Amorphous Fused Silica Surfaces. *Langmuir* **2013,** *29*, 7885-7895.
48. Hassanali, A. A.; Singer, S. J. Model for the Water−Amorphous Silica Interface: The Undissociated Surface. *J. Phys. Chem. B* **2007,** *111*, 11181-11193.
49. Hassanali, A. A.; Zhang, H.; Knight, C.; Shin, Y. K.; Singer, S. J. The Dissociated Amorphous Silica Surface: Model Development and Evaluation. *J. Chem. Theory Comput.* **2010,** *6*, 3456-3471.
50. Chen, S.-L.; Fu, L.; Gan, W.; Wang, H.-F. Homogeneous and inhomogeneous broadenings and the Voigt line shapes in the phase-resolved and intensity sum-frequency generation vibrational spectroscopy. *J. Chem. Phys.* **2016,** *144*, 034704.
51. Premadasa, U. I.; Adhikari, N. M.; Cimatu, K. L. A. Molecular Insights into the Role of Electronic Substituents on the Chemical Environment of the− CH3 and> C═ O Groups of Neat Liquid Monomers Using Sum Frequency Generation Spectroscopy. *J. Phys. Chem. C* **2019,** *123*, 28201-28209.
52. Li, D.-F.; Jiang, X.-L.; Cao, B.; Li, Z.-W.; Gao, S.-Q.; Zhou, M.; Men, Z.-W.; Zhai, N.-C. Study of asymmetric wavenumber shift of the Fermi doublet ν1 − 2ν2 in the Raman spectrum of liquid carbon disulfide. *J. Raman Spectrosc.* **2010,** *41*, 776-779.
53. Li, D.-F.; Gao, S.-Q.; Sun, C.-L.; Jiang, X.-L.; Li, Z.-W. The effect of the Fermi resonance on the Raman scattering cross sections of the Fermi doublet ν1 and 2ν2 of liquid carbon disulfide in benzene. *Spectrochim. Acta A* **2012,** *89*, 155-159.

54. Gong, N.; He, X.; Zhou, M.; He, L.; Fan, L.; Song, W.; Sun, C.; Li, Z. Effects of Fermi resonance of ν1 and 2ν2 on the Raman scattering of fundamental mode ν2 from liquid carbon disulfide. *Mater. Res. Bull.* **2017,** *85*, 104-108.
55. McHale, J. L.; Wang, C. H. Fermi resonance of Raman modes in the condensed phase: A theoretical investigation of the concentration dependent effects in molecular liquids. *J. Chem. Phys.* **1980,** *73*, 3600-3606.
56. Schwartz, M.; Moradi-Araghi, A.; Koehler, W. H. Solvent and temperature dependence of the fermi resonance parameters in methanol. *J. Mol. Struct.* **1982,** *81*, 245-252.
57. Tian, K.; Zhang, B.; Ye, S.; Luo, Y. Intermolecular Interactions at the Interface Quantified by Surface-Sensitive Second-Order Fermi Resonant Signals. *J. Phys. Chem. C* **2015,** *119*, 16587-16595.
58. Hou, J.; Zhang, X.; Lu, Z. Comparing vibrational sum frequency generation responses at fused silica and fluorite/liquid ethanol interfaces. *Chem. Phys.* **2020,** *536*, 110814.
59. Schwartz, M.; Moradi-Araghi, A.; Koehler, W. H. Fermi resonance in aqueous methanol. *J. Mol. Struct.* **1980,** *63*, 279-285.
60. Devendorf, G. S.; Hu, M.-H. A.; Ben-Amotz, D. Pressure Dependent Vibrational Fermi Resonance in Liquid CH3OH and CH2Cl2. *J. Phys. Chem. A* **1998,** *102*, 10614-10619.
61. Chase, H. M.; Ho, J.; Upshur, M. A.; Thomson, R. J.; Batista, V. S.; Geiger, F. M. Unanticipated Stickiness of α-Pinene. *The Journal of Physical Chemistry A* **2017,** *121*, 3239-3246.